

# Spatially Resolved Temperature Response Functions to CO<sub>2</sub> Emissions

Lyssa M. Freese<sup>1</sup>, Arlene M. Fiore<sup>1</sup>, Noelle E. Selin<sup>1,2</sup>

<sup>1</sup>Massachusetts Institute of Technology, Earth, Atmospheric, and Planetary Sciences

<sup>2</sup>Massachusetts Institute of Technology, Institute for Data, Systems, and Society

## Key Points:

- With a Green's Function approach, we emulate the global mean and spatially resolved temperature response to a CO<sub>2</sub> emissions trajectory.
- This approach allows expedient emulation of the spatial and temporal temperature response to varying emissions pathways.
- We illustrate this approach by evaluating local temperatures when a global mean of 2°C is reached.

---

Corresponding author: Lyssa M. Freese, [lyssamfreese@gmail.com](mailto:lyssamfreese@gmail.com)

Corresponding author: Noelle E. Selin, [selin@mit.edu](mailto:selin@mit.edu)

## Abstract

The ability to rapidly simulate the climate implications of a large number of CO<sub>2</sub> emissions trajectories is helpful for implementing mitigation and adaptation policies. A key variable of interest is near-surface air temperature, which is approximately proportional to cumulative CO<sub>2</sub> emissions. We take advantage of this relationship, diagnosing Green's Functions for the spatial temperature response to CO<sub>2</sub> emissions based on CMIP6 experiment data, creating an emulator that can be used across emissions scenarios to estimate local temperature responses. As compared to CMIP6 experiments, this approach captures the spatial temperature response with some limited accuracy in polar regions. It incorporates emissions path dependency and is useful for evaluating large ensembles of policy scenarios that are otherwise prohibitively expensive to simulate using earth system models. We apply this emulator to show differing local temperature responses when a global mean of 2°C is reached and to varying trajectories with the same cumulative emissions.

## Plain Language Summary

There is a wide range of potential pathways for future CO<sub>2</sub> emissions, and simulating them in earth system models can take large computational resources. It is important to understand the varying local impacts of different policies for effective mitigation and adaptation to climate change. A key concern is understanding local changes in temperature where people live. It is well established that the global mean temperature change is proportional to the cumulative emissions of CO<sub>2</sub>; taking advantage of this relationship, we create a simplified model that quantifies local temperature response to CO<sub>2</sub> emissions. As it takes less than one second to emulate 90 years of temperature change, this approach can be used to evaluate a multitude of policy scenarios. We evaluate this approach with the Climate Model Intercomparison Project Phase 6 (CMIP6) experiment data, showing that it captures the temperature response in different locations with some limited accuracy in polar regions. We apply this approach to show local temperature change when a global mean temperature reaches 2°C.

## 1 Introduction

Evaluating uncertainty in coupled earth-society systems is important for understanding the impact of decision-making on society, and for developing metrics such as the social cost of carbon (SCC) (Interagency Working Group on Social Cost of Greenhouse Gases, United States Government, 2021; Carleton et al., 2022). One aspect of such uncertainty analysis involves evaluating the impacts of emissions trajectories from large ensembles of social scenarios to quantify impacts on the climate system. Because of the computational cost of running full-scale earth-system models, researchers rarely use them to evaluate large numbers of different emission scenarios. Detailed information drawn from these models, however, is useful for understanding the local climate impacts of decisions.

Current methods to evaluate the temperature response of the earth system to anthropogenic emissions of CO<sub>2</sub> include running global climate models (GCMs), earth system models (ESMs), earth system models of intermediate complexity (EMICs) (Claussen et al., 2002), energy balance models (EBMs) or multi-box models that underlie many integrated assessment models (IAMs). There is a tradeoff between model complexity (and thus the detail of results) and computational cost for all of these approaches. GCMs and ESMs are too computationally expensive to run large ensembles of policy scenarios. EMICs can evaluate the spatial temperature response to CO<sub>2</sub> emissions, with smaller computational costs due to lower resolution and reduced complexity physics. EBMs are computationally inexpensive, but provide only global mean or zonally-integrated representations of temperature changes.

62 The transient climate response to cumulative emissions of carbon dioxide (TCRE)  
 63 (Matthews et al., 2009; Steinacher & Joos, 2016; Herrington & Zickfeld, 2014; Canadell  
 64 et al., 2021) can be used to calculate the temperature impact of CO<sub>2</sub> emissions. Pattern  
 65 scaling using the regional transient climate response to cumulative emissions of carbon  
 66 dioxide (RTCRES) (Leduc et al., 2016) can provide low-cost, spatially explicit estimates  
 67 of the temperature response to emissions. Applications of the RTCRES typically assume  
 68 that the pattern response of temperature is constant and insensitive to the emissions tra-  
 69 jectory, which can fail under varying emissions sizes and under reductions in emissions  
 70 (Krasting et al., 2014; Zickfeld et al., 2016; Tokarska et al., 2019). This linearity and the  
 71 TCRE have had important societal consequences, leading to the establishment of car-  
 72 bon budgets for a target global mean temperature (Meinshausen et al., 2009; Rogelj et  
 73 al., 2011; Matthews et al., 2018; Matthews & Caldeira, 2008; Drake & Henderson, 2022).

74 Response operators, or Green’s Functions, provide an alternate approach to diag-  
 75 nosing both global mean and spatial feedbacks to a forcing in ways that can capture dif-  
 76 fering pattern responses over time. Green’s Functions have been used to characterize the  
 77 radiative feedback response to sea surface temperature (Dong et al., 2019), temperature  
 78 response to CO<sub>2</sub> concentrations (Lucarini et al., 2017; Lembo et al., 2020), and atmo-  
 79 spheric transit times (Orbe et al., 2016). When diagnosed from ESMs, Green’s Functions  
 80 can form the basis for emulators that maintain the resolution of the original model, while  
 81 reducing the computational load to simulate scenarios (as seen in Geoffroy and Saint-  
 82 Martin (2014)).

83 Here, we construct an emulator, the Earth System Green’s Response emulator (ESGR),  
 84 of the pattern response of temperature to CO<sub>2</sub> emissions, which maintains the resolu-  
 85 tion of the ESMs it is derived from while enabling near-instantaneous computation. We  
 86 take advantage of the approximately linear relationship between CO<sub>2</sub> emissions and tem-  
 87 perature by diagnosing Green’s Functions for temperature response to CO<sub>2</sub> emissions,  
 88 using the Carbon Dioxide Removal Model Intercomparison Project (CDRMIP) model  
 89 output (Keller et al., 2018). ESGR is based on the multi-model mean spatial Green’s Func-  
 90 tion, and is evaluated with CMIP6 experiments. We show that it reproduces the tem-  
 91 perature response due to emissions of CO<sub>2</sub> in most locations within one standard devi-  
 92 ation of the CMIP6 multi-model mean both when CO<sub>2</sub> emissions are increasing and af-  
 93 ter their cessation. ESGR captures the time-dependent spatial patterns of the temper-  
 94 ature response under two scenarios that end with the same cumulative CO<sub>2</sub> emissions.  
 95 We illustrate how ESGR can be used to efficiently calculate metrics such as local tem-  
 96 perature changes when a global mean 2 °C is reached.

## 97 2 Methods

98 We use model output from CDRMIP to build ESGR from calculated temperature  
 99 responses to CO<sub>2</sub> emissions. Here we present the model data that is used to diagnose  
 100 the Green’s Functions and for evaluation, and explain the derivation and evaluation of  
 101 ESGR.

### 102 2.1 CMIP6 Models

103 The Earth System Grid Federation (ESGF) archive includes six models that ran  
 104 250 years of pre-industrial control simulations (*esm-pi-ctrl*), as well as 100 gigaton car-  
 105 bon (GtC) pulse (*esm-pi-CO2pulse*) and removal (*esm-pi-CDRpulse*) emission simula-  
 106 tions that branch from the *esm-pi-ctrl* at year 100 and allow the coupled carbon-climate  
 107 system to respond over 90-140 years (Keller et al., 2018). There are six models with data  
 108 from these experiments (shown in Table S1), each with two pulse scenarios (CanESM5  
 109 has 3 realizations of the pulse) for a total of 16 model runs. We compare ESGR to the  
 110 difference between the *1pctCO2* or *esm-1pct-brch-1000PgC* experiment and the *esm-pi-ctrl*  
 111 simulation for the same model source IDs as used to diagnose the Green’s Function

112 for evaluation (excluding GFDL as the data is unavaialable; see Table S2 for model in-  
113 formation).

## 114 2.2 Spatial Green's Functions

115 We diagnose Green's Functions to create a spatiotemporally resolved pattern of tem-  
116 perature response to a CO<sub>2</sub> emissions pulse. In the case of CMIP6 experiment output,  
117 the change in the response variable of interest,  $T$  (near-surface air temperature at a lo-  
118 cation  $x$ ), over time, is defined as:

$$\frac{\partial T(\mathbf{x})}{\partial t} = \mathcal{A}(T(\mathbf{x})) + E(t), \quad (1)$$

119 where  $E(t)$  is the emissions forcing, and  $\mathcal{A}(T)$  are the temperature tendency terms  
120 (everything impacting temperature aside from emissions, such as advection and radia-  
121 tion). Assuming that  $\mathcal{A}(T)$  is independent of time and linear, we define a linear oper-  
122 ator,  $\mathcal{L} \equiv \frac{\partial}{\partial t} - \mathcal{A}$ , that satisfies:

$$\mathcal{L}T(\mathbf{x}) = E(t). \quad (2)$$

123 A Green's Function,  $G(\mathbf{x}, t-t')$ , is defined as the response at location  $\mathbf{x}$  and time  
124  $t$  to an impulse (delta function) forcing at time  $t = t'$  that satisfies the linear equation:

$$\mathcal{L}G(\mathbf{x}, t-t') = \delta(t-t'), \quad (3)$$

125 If we scale this by  $E(t')$ , and then integrate this over time, the resulting equation  
126 becomes:

$$\int \mathcal{L}G(\mathbf{x}, t-t')E(t')dt' = \int E(t')\delta(t-t')dt'. \quad (4)$$

127 Taking advantage of the assumed time-independence of  $\mathcal{L}$ , and that  $\delta(t-t')$  is zero  
128 everywhere except where  $t = t'$ , we can simplify this as:

$$\mathcal{L} \left[ \int G(\mathbf{x}, t-t')E(t')dt' \right] = E(t). \quad (5)$$

129 This takes the same form as 2, allowing us to equate

$$T(\mathbf{x}, t) = \int G(\mathbf{x}, t-t')E(t')dt', \quad (6)$$

130 providing a simple equation by which we can estimate the near-surface air temperature  
131 response given an emissions time series.

## 132 2.3 Diagnosing the Green's Functions from CMIP6

133 We can take this general form of the Green's Function and apply it to the CMIP6  
134 pulse experiments. Here,  $T_p(\mathbf{x}, t; t_0)$  is the temperature change due to either the *esm-*  
135 *pi-CO2pulse* or *esm-pi-CDRpulse* experiments relative to the *pi-ctrl*, and  $E_0$  is the mag-  
136 nitude of the forcing from that pulse (100 or -100 GtC, respectively) at time  $t_0$ , result-  
137 ing in:

$$\mathcal{L}T_p = E_0\delta(t-t_0). \quad (7)$$

138 Dividing equation 7 by the constant  $E_0$ , and using equation 3 we diagnose the Green's  
139 Function

$$G(\mathbf{x}, t - t_0) = \frac{T_p(\mathbf{x}, t; t_0)}{E_0}. \quad (8)$$

140 Assuming that  $G$  does not depend on the absolute time of the pulse, we can rela-  
 141 bel the specific time  $t_0$  to any time  $t'$ , allowing us to convolve the Green's Function that  
 142 is diagnosed in equation 8 with a forcing  $E(t')$  at any time, as long as the scenario re-  
 143 mains within present  $\text{CO}_2$  states with up to 5000 GtC of cumulative emissions (as the  
 144 linear relationship has been determined to hold to this level (Tokarska et al., 2016)).

145 Practically, we construct ESGR as the multi-model mean Green's Function for ev-  
 146 ery grid box of the CMIP6 model output, equally weighting by model source ID. We use  
 147 a 4th-order polynomial fit of the Green's Function to reduce the role of unforced inter-  
 148 nal variability (see Supplementary Information for an evaluation of unforced internal vari-  
 149 ability). In order to evaluate temperature response to a given emissions scenario, we con-  
 150 volve ESGR with emissions scenarios of  $\text{CO}_2$  by summing the discretized integrands of  
 151 equation 6 (using scipy's signal convolution (Virtanen et al., 2020)).

## 152 2.4 Evaluation

153 We evaluate ESGR with the *1pctCO<sub>2</sub>* and *esm-1pct-brch-1000PgC* experiments. The  
 154 *1pctCO<sub>2</sub>* experiment prescribes a one percent increase in  $\text{CO}_2$  concentration from pre-  
 155 industrial conditions until four times the pre-industrial atmospheric concentration is reached  
 156 (Eyring et al., 2016). The *esm-1pct-brch-1000PgC* experiment follows the *1pctCO<sub>2</sub>* ex-  
 157 periment until 1000PgC has accumulated in the atmosphere after which it allows the car-  
 158 bon cycle to freely evolve with zero anthropogenic  $\text{CO}_2$  emissions.

159 We calculate the underlying emissions profiles for these two experiments accord-  
 160 ing to methods described in equation 2 of (Liddicoat et al., 2021), where the emissions  
 161 have to balance the atmospheric  $\text{CO}_2$  concentration ( $G_{ATM}$ ), exchange with the ocean  
 162 ( $S_{OCEAN}$ ), and exchange with the land ( $S_{LAND} - E_{LUC}$ ):

$$E_{CO_2} = G_{ATM} + S_{OCEAN} + (S_{LAND} - E_{LUC}) \quad (9)$$

163 Where ( $G_{ATM}$ ) is the co2mass variable, exchange with the ocean ( $S_{ocean}$ ) is fgco2,  
 164 and exchange with the land ( $S_{land} - E_{LUC}$ ) is nbp, all globally integrated.

165 The evaluation is performed by 1) convolving individual model Green's Functions  
 166 with the corresponding diagnosed *1pctCO<sub>2</sub>* and *esm-1pct-brch-1000PgC* emissions pro-  
 167 file, and 2) taking the weighted multi-model mean temperature response (weights are shown  
 168 in Table S2). We convolve ESGR for each model ID and instance with the correspond-  
 169 ing emissions and take the mean. ESGR depends in part on carbon cycle dynamics, so  
 170 it has a non-zero correlation with the emissions that underlie an individual model's fixed  
 171  $\text{CO}_2$  concentration experiments, and as a result, taking the mean before and after the  
 172 convolution yield differing results. This is only necessary in the evaluation as emissions  
 173 scenarios we independently create are not correlated to an individual model's response  
 174 and can be convolved with the ESGR multi-model mean. We compare the ESGR near-  
 175 surface air temperature response at every grid box with the weighted multi-model mean  
 176 temperature difference between the *1pctCO<sub>2</sub>* or the *esm-1pct-brch-1000PgC* experiment  
 177 and the *pi-ctrl* run.

## 178 2.5 Smoothing approach for the Green's Function

179 We reduce the role of unforced internal variability by taking the mean across mul-  
 180 tiple models (Lehner & Deser, 2023), and by using a 4th-order polynomial fit (Lehner  
 181 & Deser, 2023; Hawkins & Sutton, 2009) to the Green's Function (see Supplementary

182 Information and Figure S6 for a comparison of different fits to the Green’s Function).  
 183 The convolution also smooths out much of the high-frequency variability that is intro-  
 184 duced in the Green’s function approach (see Supplementary Information and Figure S8  
 185 for a discussion of the Fourier transform of the Green’s function, which shows the reduc-  
 186 tion of this noise).

## 187 **2.6 Transient Climate Response, Zero Emissions Commitment, and Pat-** 188 **tern Scaling Calculations**

189 We calculate a TCR for each model source ID using the temperature response of  
 190 a *1pctCO<sub>2</sub>* experiment at a doubling of CO<sub>2</sub>, defined as the mean between years 60 and  
 191 80 following the method of Matthews et al. (2009). The TCRE is the TCR divided by  
 192 the cumulative emissions to year 70 in a *1pctCO<sub>2</sub>* experiment (Matthews et al., 2009).  
 193 We use an approach similar to that of (MacDougall et al., 2020) for the ZEC, taking the  
 194 twenty-year global mean temperature anomaly centered 15 years after cessation of emis-  
 195 sions.

196 In order to pattern scale the TCRE, we multiply it by the cumulative emissions  
 197 at every time (based on Leduc et al. (2016)’s RTCRE pattern scaling).

## 198 **3 Results**

199 We first present an evaluation of ESGR with respect to global mean and pattern  
 200 response, comparing the temperature change to that of the multi-model mean CMIP6  
 201 for *1pctCO<sub>2</sub>* and *esm-1pctCO<sub>2</sub>-brch-1000PgC* experiments. We then illustrate two po-  
 202 tential applications, demonstrating how ESGR can be used for calculating the impact  
 203 of varying emissions trajectories on warming, and show that we capture the dependence  
 204 of the final state of surface temperature change on not only the cumulative emissions but  
 205 also the time-dependent emissions pathway. Importantly, this emulator takes under one  
 206 second to simulate 90 years of temperature response, which allows for the evaluation of  
 207 a multitude of emissions trajectories.

### 208 **3.1 Evaluation: Global Mean Response**

209 Figure 1a shows that the global mean time series of ESGR is positive, and has a  
 210 time mean value of 1.49°C/1000GtC, reflecting the expected warming response to emis-  
 211 sions of CO<sub>2</sub>. All of the individual model Green’s Functions have a positive time-mean  
 212 value over time, which is again expected given the positive temperature response to in-  
 213 creased CO<sub>2</sub> emissions. ESGR reproduces the global mean temperature response over  
 214 time to the *1pctCO<sub>2</sub>* and the *esm-1pctCO<sub>2</sub>-brch-1000PgC* experiments (Figure 1b). It  
 215 captures both the positive increase in temperature as a response to increasing CO<sub>2</sub> emis-  
 216 sions, and the cessation of warming when emissions are stopped under *esm-1pctCO<sub>2</sub>-brch-*  
 217 *1000PgC*.

218 We quantify ESGR’s ability to reproduce the global mean temperature change through  
 219 calculating the TCR and ZEC for both the ESGR and CMIP6 experiments (Figure 1c  
 220 and d). The multi-model mean TCR, which indicates the global mean warming after a  
 221 doubling of CO<sub>2</sub>, is 2.12°C for the CMIP6 *1pctCO<sub>2</sub>* experiments, and ESGR has a TCR  
 222 of 2.04°C. The inter-model spread of ESGR, particularly the minimum and maximum,  
 223 cover a larger range than in the CMIP6 experiments, due to the variability in ESGR’s  
 224 ability to capture global mean temperature response for individual models. The global  
 225 mean ZEC for ESGR is -0.028, indicating a slight decrease in temperature after a ces-  
 226 sation of emissions. This mean response falls within the inter-quartile range (IQR) of  
 227 the CMIP6 experiments’ ZEC; however, the mean CMIP6 ZEC indicates continued warm-  
 228 ing with a ZEC of 0.088.

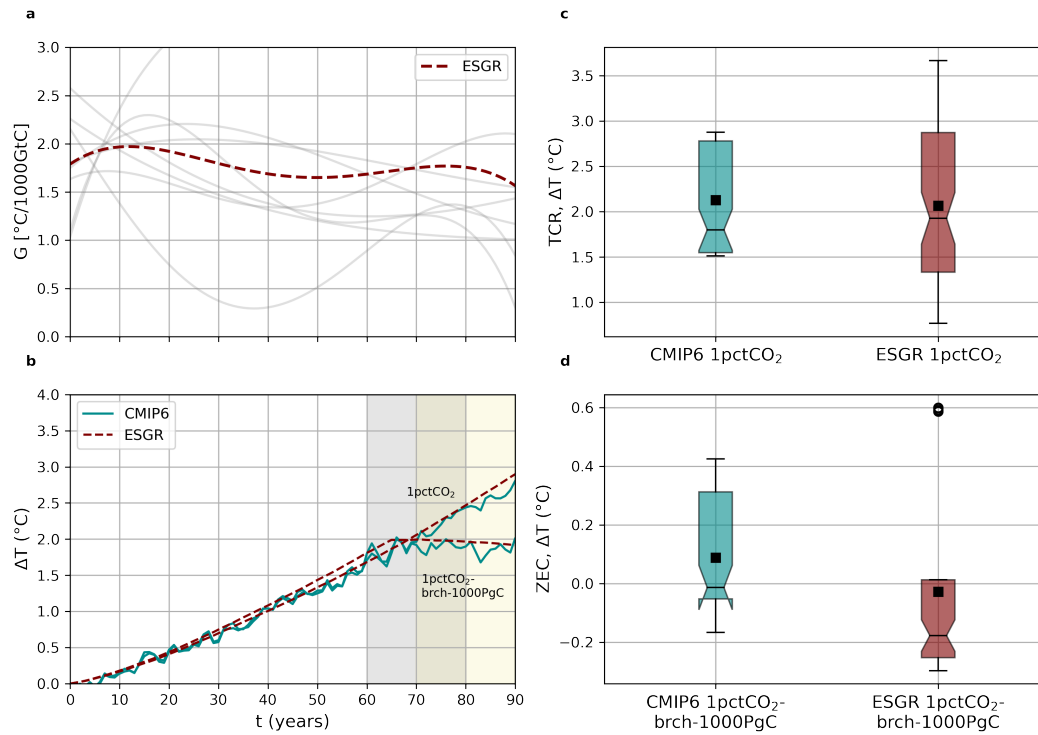


**Figure 1.** a) Global mean ESGR, and the spread of individual model Green's Functions. b) Mean of the  $1\text{pctCO}_2$  and  $esm-1\text{pctCO}_2-brch-1000\text{PgC}$  emissions convolved with ESGR as compared to the multi-model mean of the  $1\text{pctCO}_2$  and  $esm-1\text{pctCO}_2-brch-1000\text{PgC}$  model runs compared to the  $pi-ctrl$ . Grey shading indicates the 20-year averaging period to calculate the TCR, and yellow shading indicates the 20-year time averaging period to calculate the ZEC. c and d) Mean, median, and interquartile range (IQR) of the TCR and ZEC (respectively).

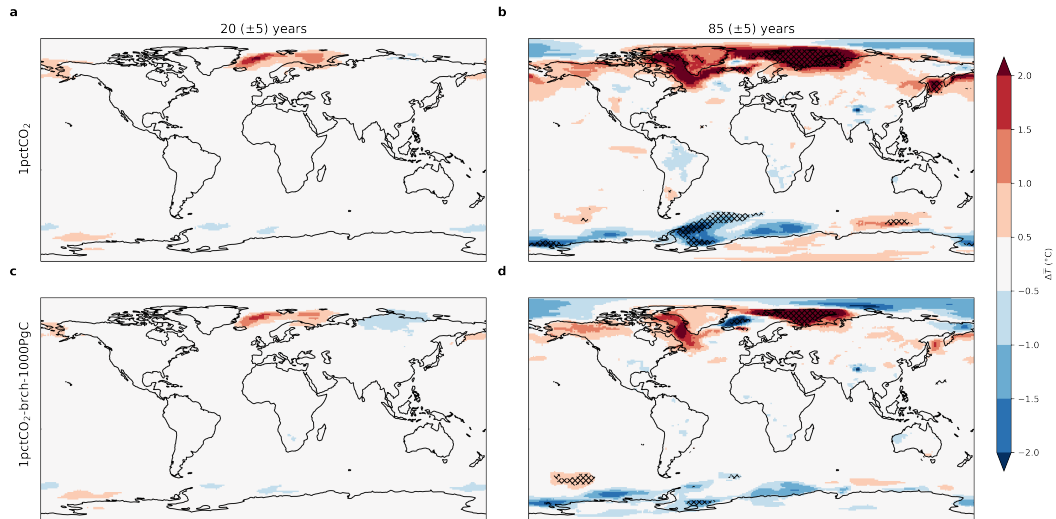


**Figure 2.** Difference in temperature response between ESGR  $1pctCO_2$  (top) or ESGR  $esm-1pct-brch-1000PgC$  (bottom) and the multi-model mean CMIP6  $1pctCO_2$  or  $esm-1pct-brch-1000PgC$  experiment at  $20(\pm 5)$  and  $85(\pm 5)$  years. Hatching indicates locations that fall outside of a  $1\sigma$  range of the model variability for the CMIP6  $1pct$  model runs.

229

### 3.2 Evaluation: Pattern Response

230

231

232

233

234

235

236

237

238

239

240

241

242

243

244

245

246

247

Figure 2 shows the difference between the pattern response of ESGR and the multi-model mean CMIP6  $1pctCO_2$  and  $esm-1pctCO_2-brch-1000PgC$  experiments at  $20(\pm 5)$  and  $85(\pm 5)$  years. ESGR is able to capture the temperature response to both  $1pctCO_2$  and  $esm-1pctCO_2-brch-1000PgC$  emissions over the first decade within  $0.5^\circ C$  of the CMIP6 model everywhere but the North Atlantic. After 20 years ESGR falls within one standard deviation of the CMIP6 model spread (Figure S5 shows the one standard deviation range), which we interpret as indicating the emulator is projecting a response consistent with the CMIP6 models. Over longer time periods, such as 85 years, ESGR is still able to capture the temperature response within  $0.5^\circ C$  of the CMIP6 experiments in all areas except for the Arctic and Antarctic due to nonlinearities from climate feedbacks (explored more in the Discussion and Conclusion). Even in the Arctic and Antarctic, many of the regions still fall within one standard deviation of the multi-model spread of CMIP6 responses; regions that are hatched are those that fall outside of this range. The temperature response in regions within one standard deviation of the multi-model mean CMIP6 responses are within the range of temperature responses that we would expect from an individual ESM. ESGR captures the reduced warming in year 85 of  $esm-1pctCO_2-brch-1000PgC$  as compared to the  $1pctCO_2$ , indicating that it can represent temperature response to both an increase and decrease in emissions (see Figure S4).

248

### 3.3 Application: Path-dependent Emissions Trajectories

249

250

251

252

253

254

255

256

ESGR can be used to show how emissions trajectories differ in their spatial temperature impact over time; here we calculate the outcomes of two example emissions scenarios that result in the same cumulative emissions. Trajectory 1 represents an increase in  $CO_2$  emissions to  $70 GtC/year$  over 20 years, followed by a rapid decline to zero  $GtC/year$  over 7 years, and Trajectory 2 represents an increase in  $CO_2$  emissions to  $37 GtC/year$  over 20 years, followed by a slow decline to zero  $GtC/year$  over 30 years. Both trajectories have the same cumulative emissions of  $1050 GtC$  over a 120-year time span (Figure 3a). We convolve ESGR with these two trajectories creating *ESGR Traj 1* and *ESGR*

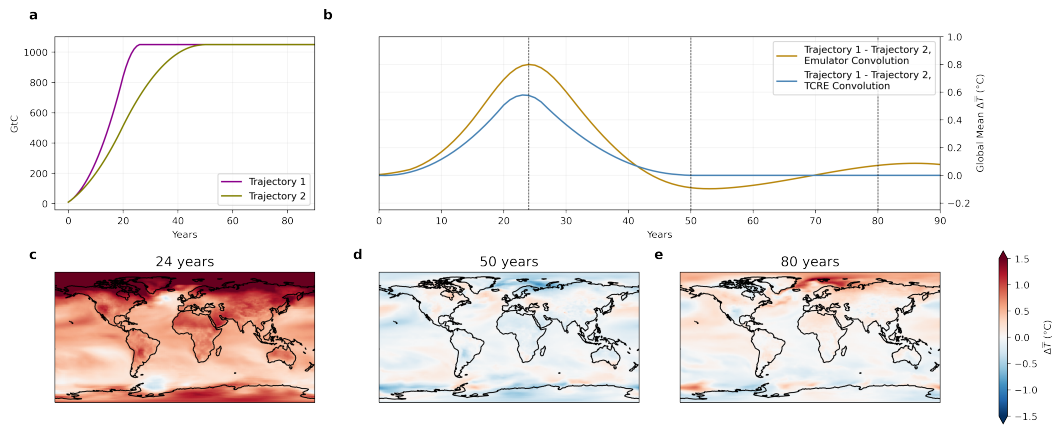


**Figure 3.** a) Cumulative emissions of CO<sub>2</sub> in GtC for 120 years in Trajectories 1 and 2. b) Global mean difference in temperature response to trajectories 1 and 2 convolved with either our Green’s Function emulator or the TCRE. Dashed lines indicate years 24, 50, and 80 which are used in part c. c) The spatial pattern of the 10-year mean temperature difference between trajectories 1 and 2 convolved with our Green’s Function emulator at years 24, 50, and 80 (all  $\pm 5$  years). The spatial pattern of temperature response by scaling the TCRE would have the same pattern of response throughout.

257 *Traj 2*. Figure 3 shows that at year 24, when the difference in cumulative emissions be-  
 258 tween the two scenarios is the greatest, there is more warming (both spatially and in the  
 259 global mean) in *ESGR Traj 1* than *ESGR Traj 2*.

260 The calculated temperature response using ESGR is different than what results from  
 261 scaling the TCRE by the cumulative emissions over time (as calculated in the Methods).  
 262 This is expected, as the TCRE does not capture temperature responses when zero emis-  
 263 sions are reached (Rogelj et al., 2018). Figure 3b shows that the peak temperature dif-  
 264 ference between Trajectories 1 and 2 is larger in ESGR than in a TCRE scaling, but the  
 265 global mean temperature response does have a similar shape, as they both have peak dif-  
 266 ferences in year 24. Once the two trajectories reach constant cumulative emissions, their  
 267 global mean temperature in the TCRE convolution are, by definition, identical. How-  
 268 ever, there are fluctuations in the difference between *ESGR Traj 1* and *ESGR Traj 2* both  
 269 in the global mean and spatially, capturing the emissions path dependency of warming  
 270 (Krasting et al., 2014).

### 271 3.4 Application: Reaching Two Degrees of Warming

272 ESGR allows us to rapidly calculate the range of temperature response at differ-  
 273 ent locations when a global mean temperature target is met under various emis-  
 274 sions trajectories. We use the *1pctCO<sub>2</sub>* and 6 additional trajectories (see Supplementary Infor-  
 275 mation) that ramp up emissions more slowly but that reach the same cumulative emis-  
 276 sions as *1pctCO<sub>2</sub>* has when the global mean temperature response is 2°C to show the  
 277 local temperature dependence on historical emissions pathways. In *ESGR 1pctCO<sub>2</sub>*, when  
 278 a 2°C global mean is reached after 69 years, Boston, Shanghai, Buenos Aires, and La-  
 279 gos are at decadal mean temperatures of 2.68°C, 2.35°C, 1.66°C, and 1.77°C, respectively.  
 280 Under scenarios that reach the same cumulative emissions by year 69, however, the decadal  
 281 mean local temperatures could range between 1.49°-2.68 °C (Boston), 1.46°-2.35 °C (Shang-  
 282 hai), 0.90°-1.66 °C (Buenos Aires), and 1.03°-1.77 °C (Lagos). The variation in final tem-  
 283 perature shows the dependency of local temperature on the trajectory of emissions. These

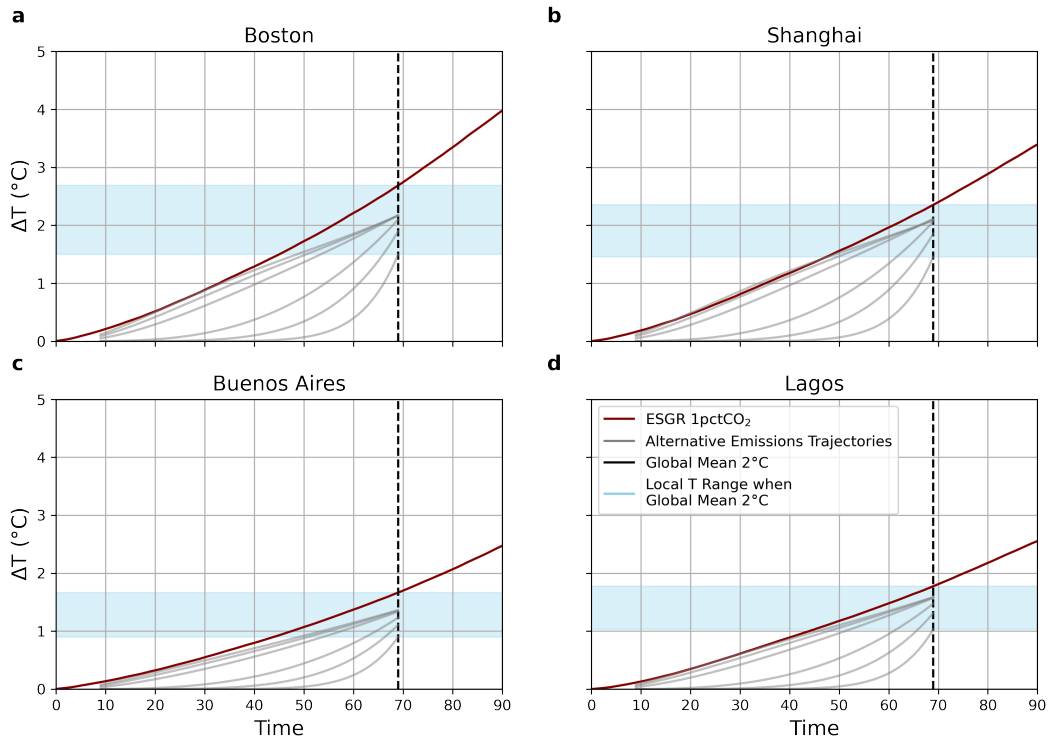


**Figure 4.** The time at which Boston, Shanghai, Buenos Aires, and Lagos reach 2 °C of warming. Black dashed lines show when the global mean temperature reaches 2°C. Horizontal blue shading indicates the local temperature range across our scenarios when a global mean of 2°C is reached. The emulated *1pctCO<sub>2</sub>* response is in maroon and light grey lines show the alternative scenarios that reach the same cumulative emissions (all shown as a ten year mean).

284 results would be strongly sensitive to the use of a scaling approach (such as pattern scal-  
 285 ing the RTCRE), as a pattern scaling would yield the exact same temperature response  
 286 in each location under the different emissions trajectories.

#### 287 4 Discussion and Conclusions

288 Understanding the relationship between global emissions and local impacts is nec-  
 289 essary for evaluating emissions trajectories under uncertainty, mitigating climate change,  
 290 and adapting to a warming world. Here, we establish a Green’s Function emulator (ESGR)  
 291 for spatially resolved temperature responses to cumulative global CO<sub>2</sub> emissions. ESGR  
 292 allows users to rapidly assess the local responses to policy options and their resulting global  
 293 CO<sub>2</sub> emissions trajectories. We evaluate this approach, which builds on the linear re-  
 294 lationships between cumulative emissions and temperature change, by identifying where  
 295 it falls within the model spread of ESM’s. We apply ESGR to two emissions trajec-  
 296 tories and use it to examine the local temperature response when the global mean reaches  
 297 2°C under multiple scenarios.

298 ESGR captures the global and local temperature response to both increases and  
 299 reductions in CO<sub>2</sub> emissions, suggesting that it reproduces the different timescales of the  
 300 radiative and carbon cycle responses. It does worst at estimating temperature response  
 301 at high latitudes, overestimating temperature changes in the Arctic, and underestim-  
 302 ating temperature changes in the Southern Ocean. Arctic amplification is the higher rate

303 of warming that is experienced in the Arctic (Pierrehumbert, 2010; Manabe & Wether-  
304 ald, 1975; Budyko, 1969; Previdi et al., 2021; Henry et al., 2021). Our overestimate in  
305 the Arctic (Figure S3), indicates that in the process of linearizing the response of the cli-  
306 mate system, we overestimate the positive feedbacks that would occur due to emissions  
307 of an additional unit of CO<sub>2</sub>, or that unforced internal variability is captured in this ap-  
308 proach. The Southern Ocean is understood to have delayed warming due to the over-  
309 turning circulation and the transport of warm waters northward (Armour et al., 2016).  
310 We either overestimate the negative feedbacks that would occur due to the emissions of  
311 an additional unit of CO<sub>2</sub>, or incorporate unforced internal variability that leads to this  
312 delayed warming, leading to an incorporation of too much Southern Ocean delayed warm-  
313 ing. Although ESGR could include unforced internal variability due to a mismatch in  
314 variability between the *pi-ctrl* and *esm-pi-CO2pulse/esm-pi-CDRpulse* experiments, we  
315 take multiple approaches to reduce the impact of this noise (see Supplementary Infor-  
316 mation).

317 ESGR can be applied to rapidly calculate metrics that can explore the implications  
318 of path dependence of local temperature response to CO<sub>2</sub>. Previous work has shown the  
319 importance of emission pathways due to nonlinearities in the climate system, particu-  
320 larly when CO<sub>2</sub> emissions are reduced after overshoot scenarios (e.g. Zickfeld et al. (2016);  
321 Tokarska et al. (2019)). Here, we are able to reproduce the path dependence of the lin-  
322 ear response of temperature to cumulative emissions (Krasting et al., 2014). One poten-  
323 tial underlying reason for this is the balance between the different spatial patterns of the  
324 fast and slow components of global warming, where a reduction in CO<sub>2</sub> forcing leads to  
325 a fast exponential response on the order of magnitude of a few years, as well as a slow,  
326 recalcitrant response that leads to up to 50% of CO<sub>2</sub> being removed from the atmosphere  
327 within 30 years, equilibration with the ocean occurring on century timescales, and weath-  
328 ering occurring on millennial timescales (Held et al., 2010; Joos et al., 2013; Denman et  
329 al., 2007; Glotter et al., 2014). ESGR is able to reproduce these fast and slow responses;  
330 the pulse of CO<sub>2</sub> it is based on causes both immediate changes in atmospheric CO<sub>2</sub> con-  
331 centration while still allowing for slow ocean carbon and heat uptake (Figure S3 shows  
332 variations in ESGR over time).

333 Many of the limitations of ESGR are due to experiments and data available from  
334 the CMIP6 archive, and based on this work we can evaluate what would be necessary  
335 to build on this approach. ESGR is built on Green's Functions derived from pulse emis-  
336 sions from a pre-industrial background state, and prior work has shown that atmospheric  
337 CO<sub>2</sub> concentration response is dependent on the background CO<sub>2</sub> concentration (Joos  
338 et al., 2013). This dependency is offset by the logarithmic relationship between CO<sub>2</sub> con-  
339 centration and radiative forcing, leading to the linear response of temperature to CO<sub>2</sub>  
340 emissions (Caldeira & Kasting, 1993). Furthermore, work has shown that this linear re-  
341 lationship between CO<sub>2</sub> cumulative emissions and temperature holds at up to 5000 GtC  
342 of cumulative emissions in ESMs (Tokarska et al., 2016). Pulses of various sizes have been  
343 shown to influence the rate of the temperature response (Steinacher & Joos, 2016). How-  
344 ever, the impact of emissions size is smaller than the impact of using various models (Krasting  
345 et al., 2014). As a result, the linear response function we derive here should be robust  
346 across varying background concentrations of CO<sub>2</sub> and emission sizes.

347 These assumptions could be better tested with additional ESM experiments to quan-  
348 tify the impact of pulse size, background state, short and long responses of the climate  
349 system, and internal variability. Additional ESM experiments pulsing varying sizes of  
350 emissions from a different starting condition would allow for quantification of the impact  
351 of the pulse size and background state—currently, the closest available experiments are  
352 the *CDR-yr2010-pulse* experiments, which are not publicly available on the Earth Sys-  
353 tem Grid Federation (ESGF) and have been run in EMICs. If the pulse (*esm-pi-CO2pulse*)  
354 and removal (*esm-pi-CDRpulse*) experiments were run for longer time periods, this would  
355 improve our ability to evaluate long timescales and estimate variations in the ZEC over

356 time (MacDougall et al., 2020). Lastly, an ensemble of pulse emissions from individual  
 357 models would allow for better quantification of the role of internal variability, and for  
 358 averaging out its impact on the Green’s Function. As climate models improve, and as  
 359 more become available, ESGR can be updated easily to reflect the latest state of the sci-  
 360 ence.

## 361 Open Research Section

362 All code to reproduce this work is available on Zenodo (currently available on github  
 363 at <https://github.com/lfreese/C02.greens>, to be updated to Zenodo for publica-  
 364 tion). The raw data from CMIP6 is available at [https://esgf-node.llnl.gov/search/  
 365 cmip6/](https://esgf-node.llnl.gov/search/cmip6/), and all of the experiments and runs used are described in Tables S1 and S2.

## 366 Acknowledgments

367 Author Contributions: Conceptualization: LF; Method development: LF; Anal-  
 368 ysis: LF; Interpretation: LF, NS, AF; Writing-original draft: LF; Writing-edits and re-  
 369 view: LF, NS, AF; Supervision: NS.

370 We thank the NIEHS Toxicology Training Grant no. T32-ES007020 and the MIT  
 371 Martin Family Society of Fellows for Sustainability (L.M.F.). This work was supported  
 372 in part by the MIT Climate Grand Challenges project “Bringing Computation to the  
 373 Climate Challenge” (L.M.F., N.E.S., and A.M.F.).

## 374 References

- 375 Armour, K. C., Marshall, J., Scott, J. R., Donohoe, A., & Newsom, E. R. (2016,  
 376 July). Southern Ocean warming delayed by circumpolar upwelling and equa-  
 377 torward transport. *Nature Geoscience*, *9*(7), 549–554. Retrieved 2023-03-28,  
 378 from <https://www.nature.com/articles/ngeo2731> (Number: 7 Publisher:  
 379 Nature Publishing Group) doi: 10.1038/ngeo2731
- 380 Budyko, M. I. (1969, January). The effect of solar radiation variations on the  
 381 climate of the Earth. , *21*(5), 611. Retrieved 2023-04-18, from [https://  
 382 a.tellusjournals.se/articles/10.3402/tellusa.v21i5.10109](https://a.tellusjournals.se/articles/10.3402/tellusa.v21i5.10109) (Number:  
 383 5 Publisher: Stockholm University Press) doi: 10.3402/tellusa.v21i5.10109
- 384 Caldeira, K., & Kasting, J. F. (1993, November). Insensitivity of global warming  
 385 potentials to carbon dioxide emission scenarios. *Nature*, *366*(6452), 251–253.  
 386 Retrieved 2023-04-18, from <https://www.nature.com/articles/366251a0>  
 387 (Number: 6452 Publisher: Nature Publishing Group) doi: 10.1038/366251a0
- 388 Canadell, J., Monteiro, P., Costa, M., da Cunha, L. C., Cox, P., Eliseev, A., ...  
 389 Zickfeld, a. K. (2021). Global Carbon and other Biogeochemical Cycles and  
 390 Feedbacks. *Climate Change 2021: The Physical Science Basis. Contribution*  
 391 *of Working Group I to the Sixth Assessment Report of the Intergovernmental*  
 392 *Panel on Climate Change*, 673–816. ([Masson-Delmotte, V., P. Zhai, A. Pirani,  
 393 S.L. Connors, C. Péan, S. Berger, N. Caud, Y. Chen, L. Goldfarb, M.I. Gomis,  
 394 M. Huang, K. Leitzell, E. Lonnoy, J.B.R. Matthews, T.K. Maycock, T. Water-  
 395 field, O. Yelekçi, R. Yu, and B. Zhou (eds.)] doi: 10.1017/9781009157896.007
- 396 Carleton, T., Jina, A., Delgado, M., Greenstone, M., Houser, T., Hsiang, S., ...  
 397 Zhang, A. T. (2022, November). Valuing the Global Mortality Consequences  
 398 of Climate Change Accounting for Adaptation Costs and Benefits. *The Quar-*  
 399 *terly Journal of Economics*, *137*(4), 2037–2105. Retrieved 2022-12-09, from  
 400 <https://doi.org/10.1093/qje/qjac020> doi: 10.1093/qje/qjac020
- 401 Claussen, M., Mysak, L., Weaver, A., Crucifix, M., Fichfet, T., Loutre, M.-F., ...  
 402 Wang, Z. (2002, March). Earth system models of intermediate complexity:  
 403 closing the gap in the spectrum of climate system models. *Climate Dynam-*

- 404 *ics*, 18(7), 579–586. Retrieved 2023-03-29, from <https://doi.org/10.1007/s00382-001-0200-1> doi: 10.1007/s00382-001-0200-1
- 405
- 406 Denman, K. L., Brasseur, G., Chidthaisong, A., Ciais, P., Cox, P. M., Dickinson,  
407 R. E., . . . Molina, M. (2007). *Couplings Between Changes in the Climate Sys-*  
408 *tem and Biogeochemistry* (Climate Change 2007: The Physical Science Basis).  
409 Cambridge University Press, Cambridge, United Kingdom and New York, NY,  
410 USA..
- 411 Dong, Y., Proistosescu, C., Armour, K., & Battisti, D. (2019). Attributing His-  
412 torical and Future Evolution of Radiative Feedbacks to Regional Warming  
413 Patterns using a Green’s Function Approach: The Preeminence of the West-  
414 ern Pacific. *Journal of Climate*, Volume 32(Issue 17). Retrieved 2022-07-  
415 08, from [https://journals.ametsoc.org/view/journals/clim/32/17/  
416 jcli-d-18-0843.1.xml](https://journals.ametsoc.org/view/journals/clim/32/17/jcli-d-18-0843.1.xml)
- 417 Drake, H. F., & Henderson, G. (2022, May). A defense of usable climate miti-  
418 gation science: how science can contribute to social movements. *Climatic*  
419 *Change*, 172(1), 10. Retrieved 2022-11-25, from [https://doi.org/10.1007/  
420 s10584-022-03347-6](https://doi.org/10.1007/s10584-022-03347-6) doi: 10.1007/s10584-022-03347-6
- 421 Eyring, V., Bony, S., Meehl, G. A., Senior, C. A., Stevens, B., Stouffer, R. J., &  
422 Taylor, K. E. (2016, May). Overview of the Coupled Model Intercomparison  
423 Project Phase 6 (CMIP6) experimental design and organization. *Geosci-*  
424 *entific Model Development*, 9(5), 1937–1958. Retrieved 2023-03-13, from  
425 <https://gmd.copernicus.org/articles/9/1937/2016/> (Publisher: Coper-  
426 nicus GmbH) doi: 10.5194/gmd-9-1937-2016
- 427 Geoffroy, O., & Saint-Martin, D. (2014, December). Pattern decomposition of the  
428 transient climate response. *Tellus A: Dynamic Meteorology and Oceanography*,  
429 66(1), 23393. Retrieved 2023-04-18, from [https://a.tellusjournals.se/  
430 article/10.3402/tellusa.v66.23393/](https://a.tellusjournals.se/article/10.3402/tellusa.v66.23393/) doi: 10.3402/tellusa.v66.23393
- 431 Glotter, M. J., Pierrehumbert, R. T., Elliott, J. W., Matteson, N. J., & Moyer,  
432 E. J. (2014, October). A simple carbon cycle representation for eco-  
433 nomic and policy analyses. *Climatic Change*, 126(3), 319–335. Retrieved  
434 2023-04-18, from <https://doi.org/10.1007/s10584-014-1224-y> doi:  
435 10.1007/s10584-014-1224-y
- 436 Hawkins, E., & Sutton, R. (2009, August). The Potential to Narrow Uncer-  
437 tainty in Regional Climate Predictions. *Bulletin of the American Meteoro-*  
438 *logical Society*, 90(8), 1095–1108. Retrieved 2023-05-30, from [https://  
439 journals.ametsoc.org/view/journals/bams/90/8/2009bams2607.1.xml](https://journals.ametsoc.org/view/journals/bams/90/8/2009bams2607.1.xml)  
440 (Publisher: American Meteorological Society Section: Bulletin of the American  
441 Meteorological Society) doi: 10.1175/2009BAMS2607.1
- 442 Held, I. M., Winton, M., Takahashi, K., Delworth, T., Zeng, F., & Vallis, G. K.  
443 (2010, May). Probing the Fast and Slow Components of Global Warming by  
444 Returning Abruptly to Preindustrial Forcing. *Journal of Climate*, 23(9), 2418–  
445 2427. Retrieved 2023-02-13, from [https://journals.ametsoc.org/view/  
446 journals/clim/23/9/2009jcli3466.1.xml](https://journals.ametsoc.org/view/journals/clim/23/9/2009jcli3466.1.xml) (Publisher: American Meteorolo-  
447 gical Society Section: Journal of Climate) doi: 10.1175/2009JCLI3466.1
- 448 Henry, M., Merlis, T. M., Lutsko, N. J., & Rose, B. E. J. (2021, March). De-  
449 composing the Drivers of Polar Amplification with a Single-Column Model.  
450 *Journal of Climate*, 34(6), 2355–2365. Retrieved 2023-04-24, from [https://  
451 journals.ametsoc.org/view/journals/clim/34/6/JCLI-D-20-0178.1.xml](https://journals.ametsoc.org/view/journals/clim/34/6/JCLI-D-20-0178.1.xml)  
452 (Publisher: American Meteorological Society Section: Journal of Climate) doi:  
453 10.1175/JCLI-D-20-0178.1
- 454 Herrington, T., & Zickfeld, K. (2014, November). Path independence of climate  
455 and carbon cycle response over a broad range of cumulative carbon emis-  
456 sions. *Earth System Dynamics*, 5(2), 409–422. Retrieved 2023-02-14, from  
457 <https://esd.copernicus.org/articles/5/409/2014/> (Publisher: Coperni-  
458 cus GmbH) doi: 10.5194/esd-5-409-2014

- 459 Interagency Working Group on Social Cost of Greenhouse Gases, United States  
 460 Government. (2021). *Technical Support Document: Social Cost of Car-*  
 461 *bon, Methane, and Nitrous Oxide.* Retrieved 2022-12-13, from [https://](https://web.archive.org/web/20221212061639/https://www.whitehouse.gov/wp-content/uploads/2021/02/TechnicalSupportDocument_SocialCostofCarbonMethaneNitrousOxide.pdf)  
 462 [web.archive.org/web/20221212061639/https://www.whitehouse](https://web.archive.org/web/20221212061639/https://www.whitehouse.gov/wp-content/uploads/2021/02/TechnicalSupportDocument_SocialCostofCarbonMethaneNitrousOxide.pdf)  
 463 [.gov/wp-content/uploads/2021/02/TechnicalSupportDocument](https://web.archive.org/web/20221212061639/https://www.whitehouse.gov/wp-content/uploads/2021/02/TechnicalSupportDocument_SocialCostofCarbonMethaneNitrousOxide.pdf)  
 464 [\\_SocialCostofCarbonMethaneNitrousOxide.pdf](https://web.archive.org/web/20221212061639/https://www.whitehouse.gov/wp-content/uploads/2021/02/TechnicalSupportDocument_SocialCostofCarbonMethaneNitrousOxide.pdf)
- 465 Joos, F., Roth, R., Fuglestedt, J. S., Peters, G. P., Enting, I. G., von Bloh, W.,  
 466 ... Weaver, A. J. (2013, March). Carbon dioxide and climate impulse re-  
 467 sponse functions for the computation of greenhouse gas metrics: a multi-model  
 468 analysis. *Atmospheric Chemistry and Physics*, *13*(5), 2793–2825. Retrieved  
 469 2020-12-16, from <https://acp.copernicus.org/articles/13/2793/2013/>  
 470 doi: 10.5194/acp-13-2793-2013
- 471 Keller, D. P., Lenton, A., Scott, V., Vaughan, N. E., Bauer, N., Ji, D., ... Zickfeld,  
 472 K. (2018, March). The Carbon Dioxide Removal Model Intercomparison  
 473 Project (CDRMIP): rationale and experimental protocol for CMIP6. *Geo-*  
 474 *scientific Model Development*, *11*(3), 1133–1160. Retrieved 2022-11-04, from  
 475 <https://gmd.copernicus.org/articles/11/1133/2018/> (Publisher: Coper-  
 476 nicus GmbH) doi: 10.5194/gmd-11-1133-2018
- 477 Krasting, J. P., Dunne, J. P., Shevliakova, E., & Stouffer, R. J. (2014).  
 478 Trajectory sensitivity of the transient climate response to cumu-  
 479 lative carbon emissions. *Geophysical Research Letters*, *41*(7),  
 480 2520–2527. Retrieved 2023-03-29, from [https://onlinelibrary](https://onlinelibrary.wiley.com/doi/abs/10.1002/2013GL059141)  
 481 [.wiley.com/doi/abs/10.1002/2013GL059141](https://onlinelibrary.wiley.com/doi/abs/10.1002/2013GL059141) (eprint:  
 482 <https://agupubs.onlinelibrary.wiley.com/doi/pdf/10.1002/2013GL059141>)  
 483 doi: 10.1002/2013GL059141
- 484 Leduc, M., Matthews, H. D., & de Elía, R. (2016, May). Regional estimates of  
 485 the transient climate response to cumulative CO<sub>2</sub> emissions. *Nature Climate*  
 486 *Change*, *6*(5), 474–478. Retrieved 2023-01-30, from [https://www.nature.com/](https://www.nature.com/articles/nclimate2913)  
 487 [articles/nclimate2913](https://www.nature.com/articles/nclimate2913) (Number: 5 Publisher: Nature Publishing Group)  
 488 doi: 10.1038/nclimate2913
- 489 Lehner, F., & Deser, C. (2023, May). Origin, importance, and predictive limits of  
 490 internal climate variability. *Environmental Research: Climate*, *2*(2), 023001.  
 491 Retrieved 2023-05-24, from <https://dx.doi.org/10.1088/2752-5295/acf30>  
 492 (Publisher: IOP Publishing) doi: 10.1088/2752-5295/acf30
- 493 Lembo, V., Lucarini, V., & Ragone, F. (2020, December). Beyond Forcing Sce-  
 494 narios: Predicting Climate Change through Response Operators in a Coupled  
 495 General Circulation Model. *Scientific Reports*, *10*(1), 8668. Retrieved 2021-  
 496 03-31, from <http://www.nature.com/articles/s41598-020-65297-2> doi:  
 497 10.1038/s41598-020-65297-2
- 498 Liddicoat, S. K., Wiltshire, A. J., Jones, C. D., Arora, V. K., Brovkin, V., Cadule,  
 499 P., ... Ziehn, T. (2021, April). Compatible Fossil Fuel CO<sub>2</sub> Emissions in the  
 500 CMIP6 Earth System Models' Historical and Shared Socioeconomic Pathway  
 501 Experiments of the Twenty-First Century. *Journal of Climate*, *34*(8), 2853–  
 502 2875. Retrieved 2022-11-04, from [https://journals.ametsoc.org/view/](https://journals.ametsoc.org/view/journals/clim/34/8/JCLI-D-19-0991.1.xml)  
 503 [journals/clim/34/8/JCLI-D-19-0991.1.xml](https://journals.ametsoc.org/view/journals/clim/34/8/JCLI-D-19-0991.1.xml) (Publisher: American Meteoro-  
 504 logical Society Section: Journal of Climate) doi: 10.1175/JCLI-D-19-0991.1
- 505 Lucarini, V., Ragone, F., & Lunkeit, F. (2017, February). Predicting Climate  
 506 Change Using Response Theory: Global Averages and Spatial Patterns.  
 507 *Journal of Statistical Physics*, *166*(3-4), 1036–1064. Retrieved 2021-03-  
 508 31, from <http://link.springer.com/10.1007/s10955-016-1506-z> doi:  
 509 10.1007/s10955-016-1506-z
- 510 MacDougall, A. H., Frölicher, T. L., Jones, C. D., Rogelj, J., Matthews, H. D., Zick-  
 511 feld, K., ... Ziehn, T. (2020, June). Is there warming in the pipeline? A  
 512 multi-model analysis of the Zero Emissions Commitment from CO<sub>2</sub>. *Bio-*  
 513 *geosciences*, *17*(11), 2987–3016. Retrieved 2023-03-15, from <https://>

- 514 [bg.copernicus.org/articles/17/2987/2020/](https://bg.copernicus.org/articles/17/2987/2020/) (Publisher: Copernicus  
515 GmbH) doi: 10.5194/bg-17-2987-2020
- 516 Manabe, S., & Wetherald, R. T. (1975, January). The Effects of Doubling  
517 the CO<sub>2</sub> Concentration on the climate of a General Circulation Model.  
518 *Journal of the Atmospheric Sciences*, 32(1), 3–15. Retrieved 2023-04-  
519 18, from [https://journals.ametsoc.org/view/journals/atsc/32/1/  
520 1520-0469\\_1975\\_032\\_0003\\_teodtc\\_2\\_0\\_co\\_2.xml](https://journals.ametsoc.org/view/journals/atsc/32/1/1520-0469_1975_032_0003_teodtc_2_0_co_2.xml) (Publisher: American  
521 Meteorological Society Section: Journal of the Atmospheric Sciences) doi:  
522 10.1175/1520-0469(1975)032<0003:TEODTC>2.0.CO;2
- 523 Matthews, H. D., & Caldeira, K. (2008). Stabilizing climate requires near-zero  
524 emissions. *Geophysical Research Letters*, 35(4). Retrieved 2022-11-04,  
525 from <https://onlinelibrary.wiley.com/doi/abs/10.1029/2007GL032388>  
526 (\_eprint: <https://onlinelibrary.wiley.com/doi/pdf/10.1029/2007GL032388>) doi:  
527 10.1029/2007GL032388
- 528 Matthews, H. D., Gillett, N. P., Stott, P. A., & Zickfeld, K. (2009, June). The  
529 proportionality of global warming to cumulative carbon emissions. *Nature*,  
530 459(7248), 829–832. Retrieved 2022-11-04, from [https://www.nature.com/  
531 articles/nature08047](https://www.nature.com/articles/nature08047) (Number: 7248 Publisher: Nature Publishing Group)  
532 doi: 10.1038/nature08047
- 533 Matthews, H. D., Zickfeld, K., Knutti, R., & Allen, M. R. (2018, January). Fo-  
534 cus on cumulative emissions, global carbon budgets and the implications for  
535 climate mitigation targets. *Environmental Research Letters*, 13(1), 010201.  
536 Retrieved 2023-02-15, from <https://dx.doi.org/10.1088/1748-9326/aa98c9>  
537 (Publisher: IOP Publishing) doi: 10.1088/1748-9326/aa98c9
- 538 Meinshausen, M., Meinshausen, N., Hare, W., Raper, S. C. B., Frieler, K., Knutti,  
539 R., . . . Allen, M. R. (2009, April). Greenhouse-gas emission targets for limiting  
540 global warming to 2 °C. *Nature*, 458(7242), 1158–1162. Retrieved 2023-04-18,  
541 from <https://www.nature.com/articles/nature08017> (Number: 7242  
542 Publisher: Nature Publishing Group) doi: 10.1038/nature08017
- 543 Orbe, C., Waugh, D. W., Newman, P. A., & Steenrod, S. (2016, October). The  
544 Transit-Time Distribution from the Northern Hemisphere Midlatitude Surface.  
545 *Journal of the Atmospheric Sciences*, 73(10), 3785–3802. Retrieved 2022-  
546 07-12, from [https://journals.ametsoc.org/view/journals/atsc/73/10/  
547 jas-d-15-0289.1.xml](https://journals.ametsoc.org/view/journals/atsc/73/10/jas-d-15-0289.1.xml) (Publisher: American Meteorological Society Section:  
548 Journal of the Atmospheric Sciences) doi: 10.1175/JAS-D-15-0289.1
- 549 Pierrehumbert, R. (2010). 4.4: Real gas radiation: basic principles. In *Principles of*  
550 *Planetary Climate*. New York: Cambridge University Press.
- 551 Previdi, M., Smith, K. L., & Polvani, L. M. (2021, September). Arctic amplification  
552 of climate change: a review of underlying mechanisms. *Environmental Research*  
553 *Letters*, 16(9), 093003. Retrieved 2023-04-24, from [https://dx.doi.org/10  
554 .1088/1748-9326/ac1c29](https://dx.doi.org/10.1088/1748-9326/ac1c29) (Publisher: IOP Publishing) doi: 10.1088/1748  
555 -9326/ac1c29
- 556 Rogelj, J., Hare, W., Lowe, J., van Vuuren, D. P., Riahi, K., Matthews, B., . . .  
557 Meinshausen, M. (2011, November). Emission pathways consistent with a  
558 2 °C global temperature limit. *Nature Climate Change*, 1(8), 413–418. Re-  
559 trieved 2023-04-18, from <https://www.nature.com/articles/nclimate1258>  
560 (Number: 8 Publisher: Nature Publishing Group) doi: 10.1038/nclimate1258
- 561 Rogelj, J., Shindell, D., Jiang, K., Fifita, S., Forster, P., Ginzburg, V., . . . Vilarinho,  
562 M. (2018). *Mitigation Pathways Compatible with 1.5°C in the Context of Sus-*  
563 *tainable Development. In: Global Warming of 1.5°C. An IPCC Special Report*  
564 *on the impacts of global warming of 1.5°C above pre-industrial levels and re-*  
565 *lated global greenhouse gas emission pathways, in the context of strengthening*  
566 *the global response to the threat of climate change, sustainable development,*  
567 *and efforts to eradicate poverty.*
- 568 Steinacher, M., & Joos, F. (2016, February). Transient Earth system responses

- 569 to cumulative carbon dioxide emissions: linearities, uncertainties, and prob-  
570 abilities in an observation-constrained model ensemble. *Biogeosciences*,  
571 *13*(4), 1071–1103. Retrieved 2023-02-14, from [https://bg.copernicus.org/](https://bg.copernicus.org/articles/13/1071/2016/bg-13-1071-2016-discussion.html)  
572 [articles/13/1071/2016/bg-13-1071-2016-discussion.html](https://bg.copernicus.org/articles/13/1071/2016/bg-13-1071-2016-discussion.html) (Publisher:  
573 Copernicus GmbH) doi: 10.5194/bg-13-1071-2016
- 574 Tokarska, K. B., Gillett, N. P., Weaver, A. J., Arora, V. K., & Eby, M. (2016,  
575 September). The climate response to five trillion tonnes of carbon. *Nature*  
576 *Nature Climate Change*, *6*(9), 851–855. Retrieved 2023-03-09, from [https://](https://www.nature.com/articles/nclimate3036)  
577 [www.nature.com/articles/nclimate3036](https://www.nature.com/articles/nclimate3036) (Number: 9 Publisher: Nature  
578 Publishing Group) doi: 10.1038/nclimate3036
- 579 Tokarska, K. B., Zickfeld, K., & Rogelj, J. (2019). Path Independence of Carbon  
580 Budgets When Meeting a Stringent Global Mean Temperature Target Af-  
581 ter an Overshoot. *Earth's Future*, *7*(12), 1283–1295. Retrieved 2023-03-24,  
582 from <https://onlinelibrary.wiley.com/doi/abs/10.1029/2019EF001312>  
583 (\_eprint: <https://onlinelibrary.wiley.com/doi/pdf/10.1029/2019EF001312>) doi:  
584 10.1029/2019EF001312
- 585 Virtanen, P., Gommers, R., Oliphant, T. E., Haberland, M., Reddy, T., Cour-  
586 napeau, D., . . . van Mulbregt, P. (2020, March). SciPy 1.0: fundamen-  
587 tal algorithms for scientific computing in Python. *Nature Methods*, *17*(3),  
588 261–272. Retrieved 2022-11-04, from [https://www.nature.com/articles/](https://www.nature.com/articles/s41592-019-0686-2)  
589 [s41592-019-0686-2](https://www.nature.com/articles/s41592-019-0686-2) (Number: 3 Publisher: Nature Publishing Group) doi:  
590 10.1038/s41592-019-0686-2
- 591 Zickfeld, K., MacDougall, A. H., & Matthews, H. D. (2016, May). On the pro-  
592 portionality between global temperature change and cumulative CO<sub>2</sub> emis-  
593 sions during periods of net negative CO<sub>2</sub> emissions. *Environmental Research*  
594 *Letters*, *11*(5), 055006. Retrieved 2023-03-24, from [https://dx.doi.org/](https://dx.doi.org/10.1088/1748-9326/11/5/055006)  
595 [10.1088/1748-9326/11/5/055006](https://dx.doi.org/10.1088/1748-9326/11/5/055006) (Publisher: IOP Publishing) doi:  
596 10.1088/1748-9326/11/5/055006